

- J.-D.; Verboom, W.; Harkema, S.; Casnati, A.; Ungaro, R.; Pochini, A.; Ugozzoli, F.; Reinhoudt, D. N. *J. Am. Chem. Soc.* **1991**, *113*, 2385. (c) Casnati, A.; Pochini, A.; Ungaro, R.; Ugozzoli, F.; Arnaud, F.; Fenni, S.; Schwing, M.-J.; Egberink, R. J. M.; de Jong, F.; Reinhoudt, D. N. *J. Am. Chem. Soc.* **1995**, *117*, 2767.
4. (a) Harrowfield, J. M.; Richmond, W. R.; Sobolev, A. N.; White, A. H. *J. Chem. Soc., Perkin Trans. 2*, **1994**, 5. (b) Beer, P. D.; Chen, Z.; Drew, M. G. B.; Gale, P. A. *J. Chem. Soc., Chem. Commun.* **1994**, 2207.
 5. Collins, E. M.; McKervey, M. A.; Madigar, E.; Moran, M. B.; Owens, M.; Ferguson, G.; Harris, S. J. *J. Chem. Soc., Perkin Trans. 1*, **1991**, 3137.
 6. Fujimoto, K.; Nishiyama, N.; Tsuzuki, H.; Shinkai, S. *J. Chem. Soc., Perkin Trans. 1*, **1992**, 643.
 7. Pouchert, C. J.; Behnke, J. *The Aldrich Library of ¹³C and ¹H FT NMR Spectra*; Aldrich Chemical Company: 1993.
 8. Gutsche, C. D.; Dhawan, B.; No, K. H.; Muthukrishnan, R. *J. Am. Chem. Soc.* **1981**, *103*, 3782.
 9. Ahn, S.; Chang, S.-K.; Kim, T.; Lee, J. W. *Chem. Lett.* **1995**, 297.
 10. Vinogradov, S. N.; Linnell, R. H. *The Hydrogen Bond*; van Nostrand Reinhold Company: New York, 1971.
 11. Groenen, L. C.; Ruel, B. H. M.; Casnati, A.; Verboom, W.; Pochini, A.; Ungaro, R.; Reinhoudt, D. N. *Tetrahedron* **1991**, *47*, 8379.
 12. Reinhoudt, D. N.; Dijkstra, P. J.; in't Veld, P. J. A.; Bugge, K. E.; Harkema, S.; Ungaro, R.; Ghidini, E. *J. Am. Chem. Soc.* **1987**, *109*, 4761.

Magnetic Property of Oxide with the Perovskite Structure, $A_2\text{Fe(III)BO}_6$ ($A=\text{Ca, Sr, Ba}$ and $B=\text{Sb, Bi}$)

Sung-Ohk Lee, Tae Yeoun Cho, and Song-Ho Byeon*

Department of Chemistry, College of Natural Sciences, Kyung Hee University, Kyung Ki 449-701, Korea
Received October 24, 1996

In the course of magnetic study on several perovskite-type oxides, $A_2\text{Fe(III)BO}_6$ ($A=\text{Ca, Sr, Ba}$, and $B=\text{Sb, Bi}$), we have observed a strong irreversibility in their dc-magnetizations. When the structural data and the Mössbauer spectra are considered, such an irreversibility is to be associated with some competitions between the nearest-neighbors (nn) and the next-nearest-neighbors (nnn) in their magnetic sublattices. Particularly, the Mössbauer spectra indicate that $\text{Sr}_2\text{FeBiO}_6$ of cubic perovskite-structure is apparently well ordered crystalline compound. Nonetheless this antiferromagnet shows a magnetic property which resembles that of a spin-glass. The strong history dependence is observed below 91 K and the irreversible magnetic behavior is also observed from the measurement of hysteresis loops at 10 K after zero-field-cooled (zfc) and field-cooled (fc) processes. Considering the nn and the nnn superexchanges of almost same order in ordered perovskite, it is proposed that there exists a competition and cancellation of antiferromagnetic and ferromagnetic superexchange between the nearest-neighbors and the next-nearest-neighbors, thus introducing a certain degree of frustration.

Introduction

Low-temperature antiferromagnetism is often observed in many compounds having the general formula $A_2\text{Fe(III)BO}_6$ where A and B are diamagnetic cations.¹ When there is a large difference in size between Fe^{3+} and B^{5+} , the materials adopt a perovskite-related structure with an alternate ordering of the cations B^{5+} and Fe^{3+} on the octahedral sites.² The magnetic Fe^{3+} ions ($3d^5: {}^6A_{1g}$) thus form a face-centered array in a cubic unit cell having $a_0 \approx 8 \text{ \AA}$, that is $2a_p$ where a_p is the cell parameter of the primitive perovskite unit cell.

Several years ago, we reported the synthesis of $\text{Sr}_2\text{FeBiO}_6$ and $\text{Ba}_2\text{FeBiO}_6$ under the high oxygen pressure.^{3,4} The strong superstructure lines in powder X-ray diffraction pattern of $\text{Sr}_2\text{FeBiO}_6$ showed an ordered perovskite with a double unit cell parameter. The weak extra reflections in $\text{Ba}_2\text{FeBiO}_6$ also lead to an indexation with a pseudocubic unit cell parameter. The inverse of zero-field-cooled magnetic susceptibilities of both compounds in the high-tem-

perature range obeyed typical Curie-Weiss law

$$\chi = C / (T - \theta)$$

with Curie paramagnetic constant $C \approx 4.6 \text{ emu.K/mol}$ implying a spin value of $S=5/2$ as expected for high-spin Fe^{3+} . Quite largely negative Curie temperature indicated predominant antiferromagnetic exchange interactions between the Fe moments. However, a marked deviation from the linearity below about 200 K was observed in both two compounds. Nevertheless the ^{57}Fe Mössbauer spectra of $\text{Sr}_2\text{FeBiO}_6$ at 80 K showed a superposition of a magnetic hyperfine sextuplet and a paramagnetic singlet, which was explained to result from slow relaxation process in long-range superexchange. Such experimental results of magnetic susceptibility and the Mössbauer effect allowed us to conclude that the antiferromagnetic long-range ordering is induced below 91 K with $\text{Sr}_2\text{FeBiO}_6$.

In view of the magnetic study of these compounds our main interest has been focussed on a strong deviation of

magnetic susceptibility data from Curie-Weiss law in low temperature range. Since this behavior seemed to indicate the appearance of magnetic correlations which is associated with freezing phenomena of the Fe^{3+} magnetic moments, we have measured the dependence of magnetic moment on their magnetic history. During the low-field measurements of these compounds, a remarkable magnetic irreversibility was observed in both two compounds and particularly an interesting magnetic property similar to that of typical spin-glass system was observed in $\text{Sr}_2\text{FeBiO}_6$. In this paper we discuss, from field dependence of magnetic susceptibility and hysteresis loop measurements, that a spin-glass like behavior in crystallographically well ordered perovskite could arise from a competition of antiferromagnetic and ferromagnetic superexchange between the nearest-neighbors and the next-nearest-neighbors. For comparison with the structure and the magnetic property of similar Fe(III) compounds, A_2FeSbO_6 ($A=\text{Ca}$, Sr , and Ba)⁵ were also prepared and compared.

Experimental

A_2FeSbO_6 ($A=\text{Ca}$, Sr , and Ba) were obtained from the stoichiometric mixtures of $\text{A}(\text{NO}_3)_2$, Fe_2O_3 , and Sb_2O_5 . These mixtures were calcined at 800 °C in air and then heated at 900-1000 °C for 48 h under the oxygen current.

$\text{Sr}_2\text{FeBiO}_6$ and $\text{Ba}_2\text{FeBiO}_6$ were synthesized by a solid state reaction as previous description.^{3,4} The stoichiometric mixture of $\text{Sr}(\text{CH}_3\text{COO})_2$, Bi_2O_3 , and $\text{Fe}(\text{NO}_3)_3 \cdot 9\text{H}_2\text{O}$ was decomposed in air and heated at 1000 °C. Final oxygen pressure treatment (7.5 and 4 GPa for $\text{Sr}_2\text{FeBiO}_6$ and $\text{Ba}_2\text{FeBiO}_6$, respectively) were performed at 1000 °C for 10 min using belt-type apparatus. The oxygen gas was generated *in-situ* by a decomposition of KClO_3 and remaining KCl after the reaction was leached out by distilled water.

Powder X-ray diffraction data were recorded on a rotating anode installed M18XHF MACScience diffractometer using $\text{Cu K}\alpha$ radiation monochromatized by the curved graphite. The data for Rietveld analysis were collected with a step-scan procedure in the range $2\theta=20^\circ$ to 120° with counts for a second at 0.02° intervals. The fitting of reflection positions and intensities were carried out using Rietveld analysis program RIETAN(Macintosh version).⁶

The Mössbauer data were collected at room temperature using a 1.11 GBq $^{57}\text{Co}/\text{Rh}$ source matrix held at room temperature by an Austin Science S-600 Mössbauer spectrometer. The curve fitting of the obtained spectra was performed with a personal computer, assuming that the spectra were composed of peaks in Lorentzian line shape. Isomer shifts are quoted relative to the centroid of the spectrum of iron metal at room temperature.

dc-susceptibility and magnetic hysteresis data were measured with a Quantum Design SQUID magnetometer. The earth's field was shielded. The powder sample held in a gellatin capsule was first cooled in zero-applied-field (*zfc* curve) down to 5 K. The magnetic field of 1 kOe was applied and held constant. Measurements were taken at increasing temperatures up to 300 K. Then the sample was cooled down again at the field of 0.1, 0.5, 1, 5, and 10 kOe and measured at the same fields as applied during field-cooled process (*fc* curve). Hysteresis loops of $\text{Sr}_2\text{FeBiO}_6$ were

measured at 10 K after zero-field-cool and field-cool ($H=1$ kOe) with magnetic field sweeping from -2 to 2 kOe.

Results and Discussion

The powder X-ray diffraction patterns of the title compounds showed several different symmetries depending on the A or B cations. The estimated crystal symmetries and unit cell parameters are listed in Table 1. $\text{Ca}_2\text{FeSbO}_6$ was previously⁵ described as an orthorhombic structure, but it appears that the starting refinement using this symmetry was not close enough to the correct values for the least-squares program to converge on the true minimum. On the while our new data could be fitted with an acceptable reliability factors (Table 2) to a monoclinic ($P2_1/n$) symmetry in which Fe and Sb are ordered.⁷ The diffraction intensity data of $\text{Ba}_2\text{FeSbO}_6$ was refined on the basis of hexagonal symmetry rather than the cubic or pseudocubic. Differently from previous report,⁵ any superstructure reflections with indices ($003n$) were not observed in the diffraction pattern of $\text{Ba}_2\text{FeSbO}_6$. The cubic perovskite structure ideally requires $(r_A+r_O)=\sqrt{2}(r_B+r_O)$, and a ratio r_B/r_A much in excess of this ideal leads to the introduction of hexagonal stacking among the close-packed AO_3 layers. Figure 1 shows a typical 6H-hexagonal structure ($P6_3/mmc$) with a *cch* stacking sequence for the close-packed BaO_3 layers. In this structure, the 6-coordinate cations lie either in an B_2O_6 dimer or in a single corner-shared octahedron that links different dimers together. If all the dimers with short cation-cation distance consist of different cations, therefore, some of ($003n$) reflections are generally present. An absence of such reflections indicates that the layers of cations perpendicular to the hexagonal axis are not alternately occupied by Fe and Sb. In this disordered structure, however, the cation repulsion in $\text{Sb}^{5+}\text{-Sb}^{5+}$ pairs will be much stronger than in $\text{Fe}^{3+}\text{-Sb}^{5+}$ and $\text{Fe}^{3+}\text{-Fe}^{3+}$ pairs. It is consequently probable that only 1/2 of $4f$ positions and 2/3 of $2a$ positions are oc-

Table 1. The crystal symmetry and unit cell parameters of some Fe(III) compounds

| Com-pounds | Symmetry | Unit cell parameters (Å) | | | |
|-----------------------------|-------------|--------------------------|-----------|------------|-------------|
| | | a (Å) | b (Å) | c (Å) | β (°) |
| $\text{Ca}_2\text{FeSbO}_6$ | monoclinic | 5.4371(1) | 5.5259(1) | 7.7340(2) | 89.97(1) |
| $\text{Sr}_2\text{FeSbO}_6$ | cubic | 7.9098(2) | | | |
| $\text{Ba}_2\text{FeSbO}_6$ | hexagonal | 5.7825(2) | | 14.2046(5) | |
| $\text{Sr}_2\text{FeBiO}_6$ | cubic | 8.063(2) | | | |
| $\text{Ba}_2\text{FeBiO}_6$ | pseudocubic | 8.279(2) | | | |

Table 2. Structure parameters of $\text{Ca}_2\text{FeSbO}_6$ at room temperature (space group $P2_1/n$)

| Atom | occupancy | x | y | z | B_{iso} (Å ²) |
|------|-----------|-----------|-----------|-----------|------------------------------------|
| Ca | 1.0 | 0.0085(2) | 0.0435(5) | 0.2511(8) | 0.58(7) |
| Fe | 1.0 | 0.5 | 0.0 | 0.0 | 0.82(6) |
| Sb | 1.0 | 0.0 | 0.5 | 0.0 | 0.47(4) |
| O1 | 1.0 | 0.305(3) | 0.293(3) | 0.045(4) | 0.9(5) |
| O2 | 1.0 | 0.289(3) | 0.298(3) | 0.464(5) | 0.4(6) |
| O3 | 1.0 | 0.915(3) | 0.475(2) | 0.252(3) | 0.9(4) |

$$R_w=9.75\%, R_f=2.64\%, R_p=7.04\%, R_g=5.60\%$$

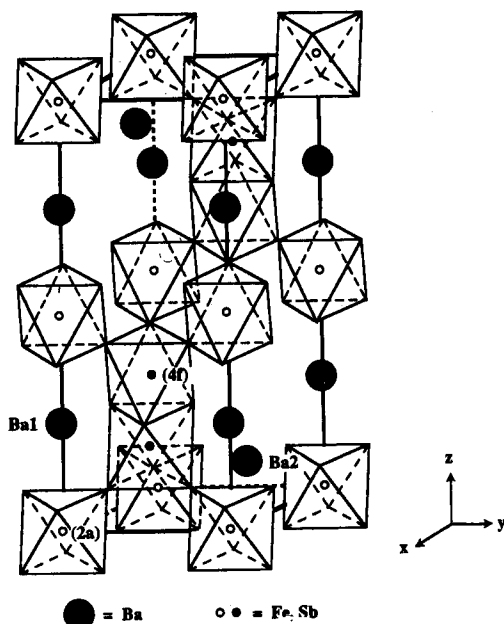


Figure 1. The 6H-perovskite structure of $\text{Ba}_2\text{FeSbO}_6$. Fe and Sb atoms randomly occupy the 2a and 4f sites. Hatched circles are Ba atoms.

occupied by Sb in order to avoid the formation of unfavorable $\text{Sb}^{5+}\text{-Sb}^{5+}$ pairs. Unfortunately, such a distribution could not be confirmed by the intensity data of polycrystalline sample. $\text{Sr}_2\text{FeSbO}_6$ and $\text{Sr}_2\text{FeBiO}_6$ have cubic structures as previously determined.^{4,5} The existence of superstructure reflections gave double unit cell parameters. A weak local distortion of the FeO_6 octahedron would be expected by a broadening of the diffraction lines and observation of very weak superstructure reflections in pseudocubic $\text{Ba}_2\text{FeBiO}_6$. Due to too small amount (less than 50 mg) of product obtained by 'belt' type experiment, the extent of partial ordering and local distortion of the FeO_6 octahedron in $\text{Ba}_2\text{FeBiO}_6$ could not be estimated. As will be discussed below, the Mössbauer spectrum of $\text{Sr}_2\text{FeSbO}_6$ showed two types of Fe^{3+} site, one being pure octahedron and the other distorted octahedron. Since such an observation seemed to result from the significant partial disordering, the Rietveld refinement was carried out for $\text{Sr}_2\text{FeSbO}_6$. The final minimum reliability factor (Table 3) and agreeable isotropic temperature factors were obtained when the octahedral sites are predominantly occupied by Fe^{3+} and Sb^{5+} ions in 1:1 ordered manner, but about 12% concentration of two cations are randomly distributed.⁷

Figure 2 shows the ^{57}Fe Mössbauer spectra of $\text{Sr}_2\text{FeSbO}_6$, $\text{Sr}_2\text{FeBiO}_6$, and $\text{Ba}_2\text{FeBiO}_6$ at room temperature. The isomer shift value of 0.421 mm/s ($\text{Sr}_2\text{FeSbO}_6$), 0.389 mm/s ($\text{Sr}_2\text{FeBiO}_6$), and 0.407 mm/s ($\text{Ba}_2\text{FeBiO}_6$) are typical for high-spin Fe(III). The observed quadrupole splitting indicates a cooperative local structural distortion of the FeO_6 octahedra in $\text{Ba}_2\text{FeBiO}_6$ as expected by the X-ray diffraction study. But very small splitting (0.349 mm/s) and very narrow line (line width=0.389 mm/s) are consistent with a predominant crystallographic ordering between Fe and Bi. In the spectrum of $\text{Sr}_2\text{FeSbO}_6$, another quadrupole doublet (isomer shift=0.408 mm/s, quadrupole splitting=0.746 mm/s) is su-

Table 3. Structure parameters of $\text{Sr}_2\text{FeSbO}_6$ at room temperature (space group $\text{Fm}\bar{3}\text{m}$)

| Atom | occupancy | x | y | z | B_{iso} (\AA^2) |
|------|-----------|----------|------|------|-------------------------------------|
| Sr | 1.0 | 0.25 | 0.25 | 0.25 | 0.66(2) |
| Fe1 | 0.88 | 0.0 | 0.0 | 0.0 | 0.79(8) |
| Fe2 | 0.12 | 0.5 | 0.5 | 0.5 | 0.79(8) |
| Sb1 | 0.88 | 0.5 | 0.5 | 0.5 | 0.52(2) |
| Sb2 | 0.12 | 0.0 | 0.0 | 0.0 | 0.52(2) |
| O | 1.0 | 0.249(3) | 0.0 | 0.0 | 1.8(7) |

$$R_{\text{wp}}=11.25\%, R_{\text{I}}=2.75\%, R_{\text{p}}=7.71\%, R_{\text{E}}=4.60\%$$

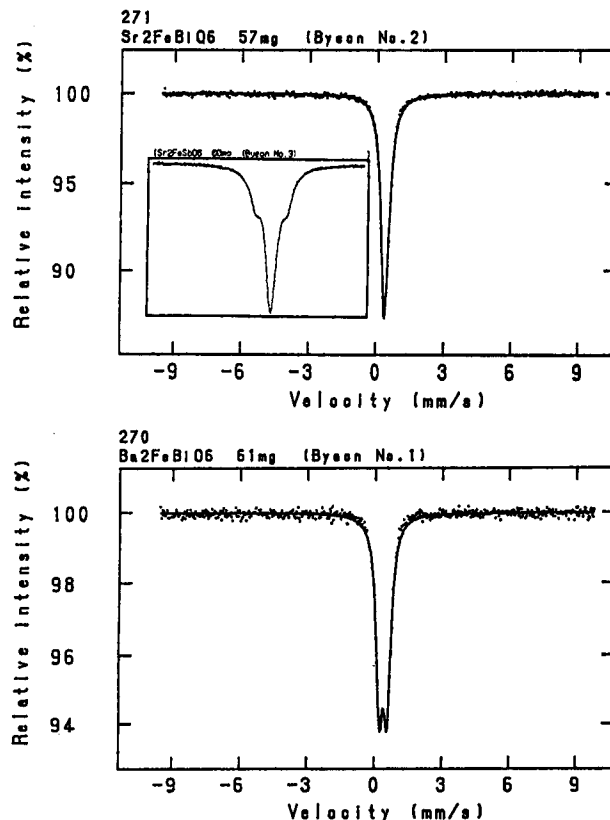


Figure 2. Mössbauer spectra of $\text{Sr}_2\text{FeBiO}_6$ (top) and $\text{Ba}_2\text{FeBiO}_6$ (bottom) at room temperature. Inset shows the spectra of $\text{Sr}_2\text{FeSbO}_6$. The isomer shift is 0.389 mm/s ($\text{Sr}_2\text{FeBiO}_6$), 0.407 mm/s ($\text{Ba}_2\text{FeBiO}_6$), and 0.421 mm/s ($\text{Sr}_2\text{FeSbO}_6$). The quadrupole splitting is 0.349 mm/s and 0.746 mm/s for $\text{Ba}_2\text{FeBiO}_6$ and $\text{Sr}_2\text{FeSbO}_6$, respectively.

perposed on the singlet centered at 0.421 mm/s. This broad doublet would be induced by some disordering between Fe and Sb. Compared with the narrow singlet, about 17% intensity of broad doublet is in agreement with the result of the Rietveld refinement for $\text{Sr}_2\text{FeSbO}_6$.

In Figure 3, we show the reciprocal zero-field-cooled susceptibilities of several Fe(III) oxides from 5 K up to room temperature. In the high temperature regime the magnetic susceptibilities display typical Curie-Weiss behavior, obtained paramagnetic moments of 5.6-6.0 μ_{B} and Curie temperatures $\theta = -70 \sim -800$ K being in agreement with the results of previous works.³⁻⁵ The values of the magnetic moments are close to the theoretical 5.92 μ_{B} spin-only high-

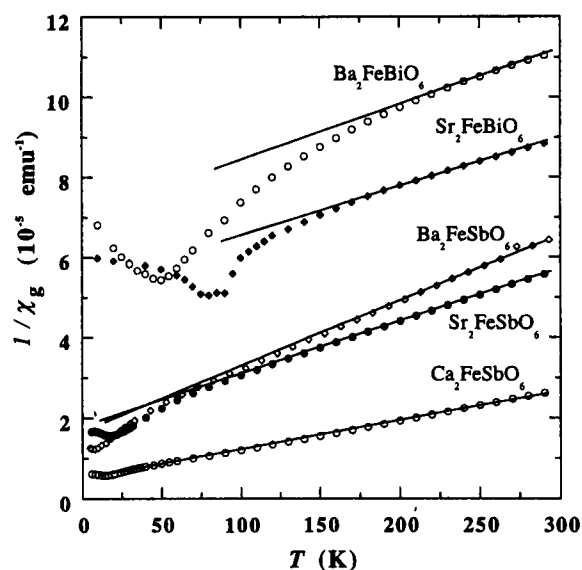


Figure 3. Inverse dc-magnetic susceptibility as a function of the temperature. The solid lines represent high-temperature asymptotic Curie-Weiss behavior.

spin value of Fe^{3+} ions, which are consistent with the spin-state expected from the isomer shift in the Mössbauer spectra. The negative sign of the Curie temperature suggests that the dominant interactions between the Fe(III) magnetic moments are antiferromagnetic. Of interest to us is the fact that a marked deviation from the linearity occurs in wide temperature range for all compounds, seeming to signal the appearance of magnetic correlations among the Fe(III) magnetic moments. This deviation increases with decreasing temperature and then a peak appears, which is associated with an ordering of the Fe(III) magnetic moment. Below this temperature, the magnetic irreversibility starts and the behavior of the sample depends on its magnetic history, leading to the differences observed in the *zfc* and the *fc* susceptibilities shown in Figure 4.

In order to explain such magnetic behaviors of common perovskite oxides, it is helpful to compare the surroundings of the magnetic cation in ordered and disordered structure. If we consider the antiferromagnetic interactions between six nearest-neighbors (*nn*) at a distance a_p (the type G magnetic order) of magnetic cluster in disordered structure, the interaction between 12 next-nearest-neighbors (*nnn*) at a distance $\sqrt{2}a_p$ is ferromagnetic as shown in Figure 5-a. In ordered structure, on the contrary, the *nnn* interaction at a distance $2a_p$ is ferromagnetic if the *nn* interaction at a distance $\sqrt{2}a_p$ is antiferromagnetic as shown in Figure 5-b. Partial disordering reduces the number of magnetic *nnn* pairs (separation $2a_p$) in ordered structure, whilst increasing the number of magnetic *nn* pairs (separation a_p) in disordered one. This magnetic sublattice (more than 10%) favors ferromagnetic coupling between cations a distance $\sqrt{2}a_p$ apart rather than antiferromagnetic. Although the principal (about 90%) magnetic superexchange is still between cations separated by a distance $2a_p$, such an effect may introduce a certain degree of spin frustration. The high temperature clusters are likely to carry an uncompensated magnetic moment, the orientation of which will be influenced by an ex-

ternal field as shown by the observed variation of susceptibility of $\text{Sr}_2\text{FeSbO}_6$ on cooling in a field and in zero field. The FeO_6 octahedra are cooperatively distorted in $\text{Ba}_2\text{FeBiO}_6$ (as suggested in its Mössbauer spectrum) and $\text{Ca}_2\text{FeSbO}_6$. Therefore, a slight magnetic anisotropy as well as partial disordering could be responsible for the magnetic irreversibility.

The magnetic property of $\text{Ba}_2\text{FeSbO}_6$ would be explained by considering the characteristics of 6H-perovskite structure. In this structure, magnetic cations occupy both corner-shared and face-shared octahedra. The exchange constant for coupling between corner-shared and face-shared sites is lower than that for pairs of face-shared sites and these magnetic cations are likely to be paramagnetic at high temperature. However, they may well be responsible for the unusual behavior of the susceptibility which is observed below 50 K. The divergence of the *zfc* and the *fc* data indicates that either a weak ferromagnetism or magnetic clusters with an uncompensated magnetic moment are present. This is to be associated with any particular Fe_2O_3 dimer that shares corner with a statistical distribution of SbO_6 and FeO_6 octahedra. The observed susceptibility is a summation over all the possible combinations. At temperature low enough for antiferromagnetic coupling between face-shared and corner-shared sites to become significant it will undoubtedly include a contribution from extended clusters containing an odd number of Fe(III) cations which will therefore carry an uncompensated magnetic moment. The presence of magnetic cations on the corner-shared sites provides a mechanism for magnetic coupling between dimers and as the temperature is lowered we would expect local magnetic coupling to develop into long-range antiferromagnetic order. Similar arguments have been used to account for the behavior of other disordered magnetically diluted systems.⁸

A remarkable magnetic irreversibility is also observed with $\text{Sr}_2\text{FeBiO}_6$. Even though the magnetic susceptibilities of $\text{Sr}_2\text{FeBiO}_6$ were measured at lower applied field, no maximum was observed as shown in Figure 6. Thus small fields were sufficient to destroy the antiferromagnetism in the material. Further evidence of irreversible behavior at low temperatures comes from the hysteresis data of Figure 7 which indicates a remanent moment when the *zfc* sample is demagnetized at 10 K. The hysteresis loop is shifted to higher values when the sample is cooled at 1 kOe field. All of the above resembles a transition to spin-frozen state below 91 K.

It has long been believed that frustration and disorder are the essential conditions for obtaining a spin-glass state.⁹⁻¹¹ The disorder in the distribution of magnetic interactions may be either topological or may arise from a random magnetic dilution in crystalline materials. Similar magnetic property was observed in an antiferromagnetic non-frustrated lattice, $\text{Sr}_2\text{FeNbO}_6$.¹² In that case Fe^{3+} and non-magnetic Nb^{5+} are randomly distributed in the corner-shared octahedral site, forming a diluted simple cubic lattice. Magnetically non-diluted spin-glass system is rare but exist.^{13,14} Certain spin-glass properties were also observed in ordered crystalline solids such as ordered pyrochlore which is highly frustrated.^{15,16} What is remarkable about our results is that $\text{Sr}_2\text{FeBiO}_6$ is apparently well ordered crystalline perovskite. From strong superstructure peaks in powder X-ray dif-

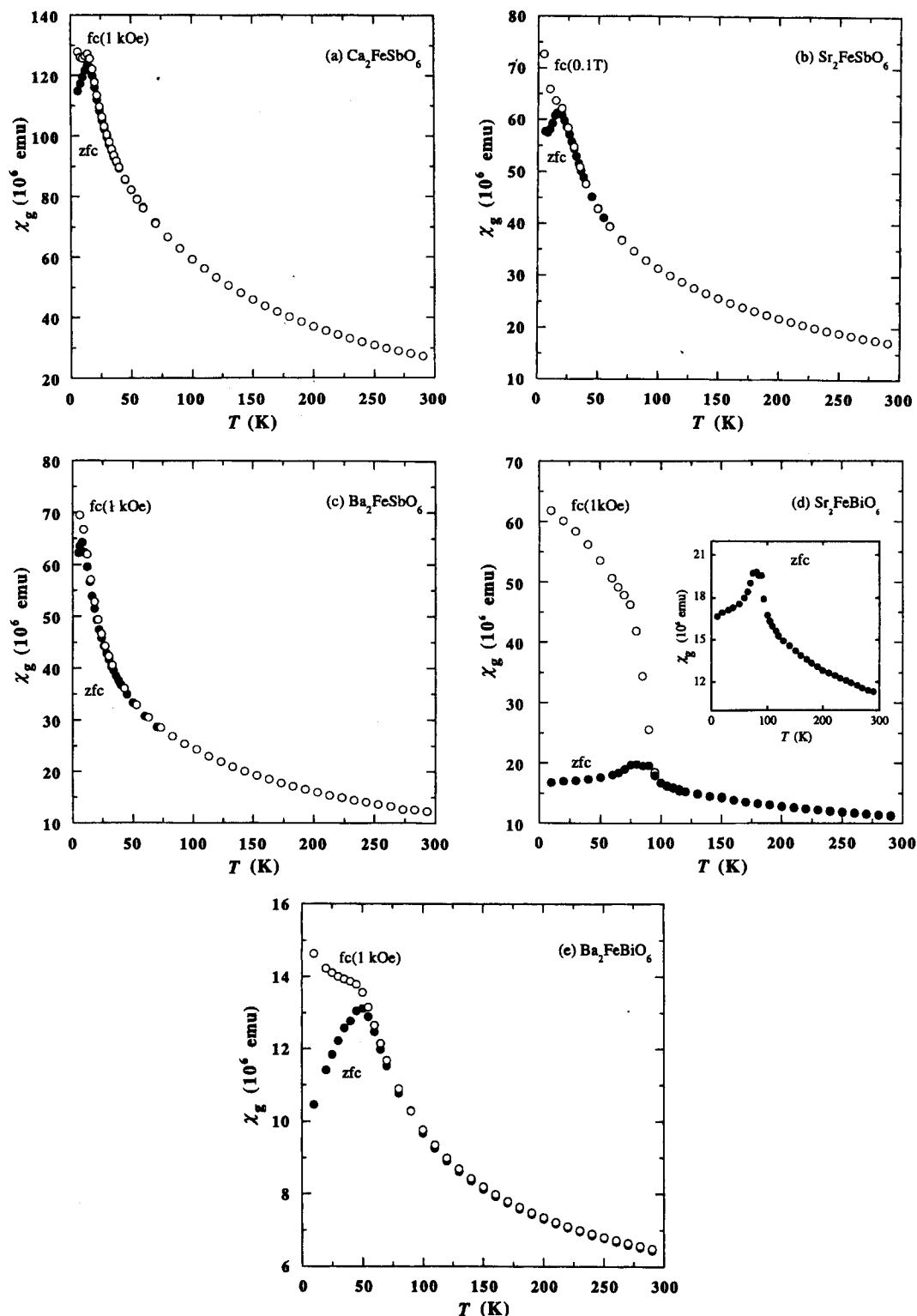


Figure 4. dc-magnetic susceptibilities measured at constant field ($H=1$ kOe) after field-cooled (*fc*) and zero-field-cooled (*zfc*) processes. The inset of 4-d shows a zero-field-cooled susceptibility data.

fraction pattern and narrow singlet line in the Mössbauer spectrum, the crystal structure of $\text{Sr}_2\text{FeBiO}_6$ is consistent with the cubic perovskite structure in which Fe^{3+} and Bi^{3+} fully occupy the ideal crystallographic sites with an ordered manner. Nonetheless a magnetic phase transition is observed

below 91 K which resembles that of a spin-glass. The six-coordinate Fe^{3+} has the electronic structure $t_{2g}^3 e_g^2$ and hence there can be π -contribution to the superexchange. Since the mechanism for 90° superexchange must occur *via* π -bonding (see Figure 5-a), the *nn* antiferromagnetic interactions in

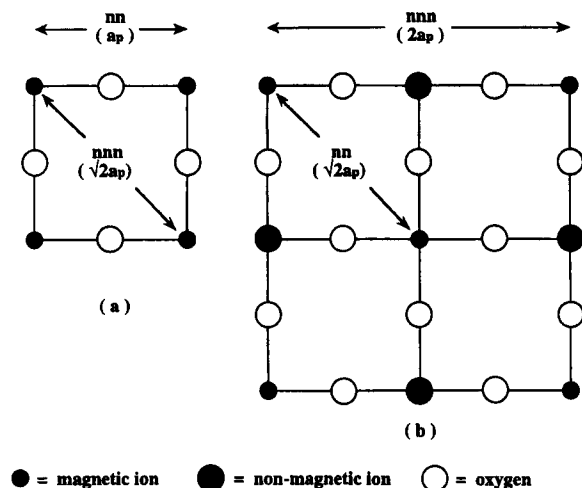


Figure 5. The magnetic sublattice of the disordered cluster (a) and the ordered structure (b). a_p represents the cell parameter of the primitive perovskite unit cell.

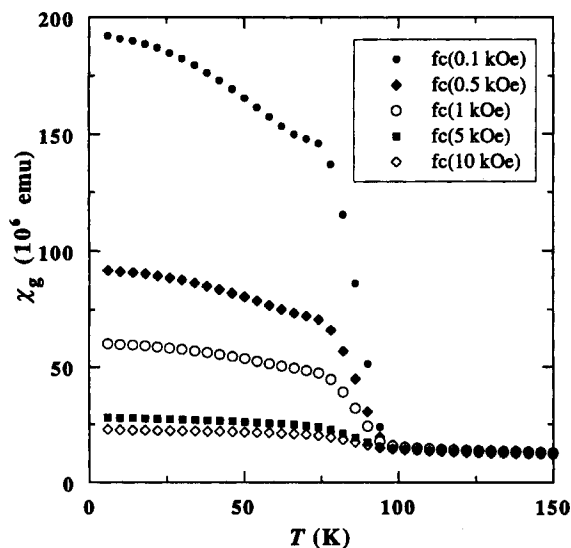


Figure 6. dc-magnetic susceptibilities of $\text{Sr}_2\text{FeBiO}_6$ measured after field-cooled processes at different applied fields.

simple cubic perovskite lattices are two orders of magnitude greater than the nnn interactions.¹⁷ This does not seem to be the case in ordered perovskite antiferromagnets. As indicated by Blasse,¹⁸ the $6s$, $6p$, and $6d$ empty orbitals of Bi^{5+} with $5d^{10}$ electronic configuration are available for molecular-orbital formation. A band calculation¹⁹ predicted that $\text{Bi}6s\text{-O}2p$ orbital overlap will be very effective in the perovskite lattice. The lowering of the vacant energy levels on the diamagnetic 6-coordinate Bi^{5+} would enable these d^{10} orbitals to play a greater role in the magnetic superexchange. While 90° Fe-O-Bi-O-Fe exchange is only possible via π -bonding with contribution of the $6p$ orbital (see Figure 5-b), such mechanism can also occur via σ -bonding alone if the $6s$ orbital is used. This indicates that the strength of a superexchange through the paths of O-Bi-O with the angle of 90° (nn) and 180° (nnn) could be about same order. Thus no fundamental difference exists between 90° and 180° su-

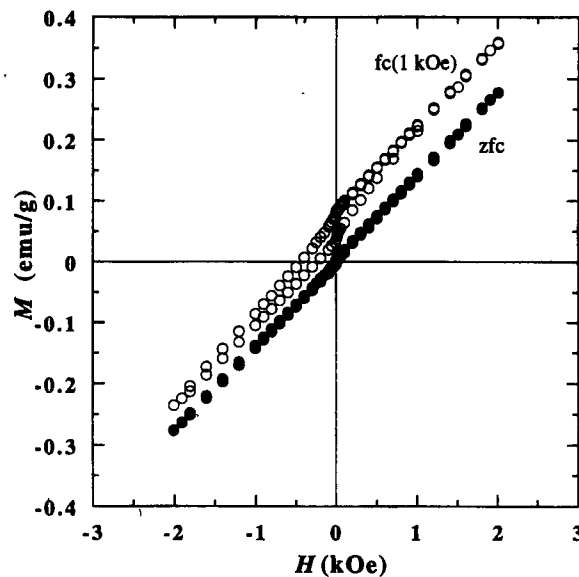


Figure 7. Hysteresis loops of $\text{Sr}_2\text{FeBiO}_6$ measured at $T=10$ K after zero-field-cooled and field-cooled ($H=1$ kOe) processes (magnetic field sweeping from -2 to 2 kOe).

perexchange in ordered perovskite. For instance, the type IIIa ordering adopted by $\text{Ba}_2\text{LaRuO}_6$ is consistent with a strong nn interaction over a distance of $\sqrt{2}a_p$ (90°), but in this case there is also a significant antiferromagnetic nnn interaction over a distance of $2a_p$ (180°).²⁰ From this view point, the frustration could arise from the competition and cancellation of antiferromagnetic and ferromagnetic superexchange between the nearest-neighbors and the next-nearest-neighbors through different paths involving O-Bi-O intermediary in ordered cubic perovskite lattice. A strong deviation from Curie-Weiss law at high temperature would indicate considerable short range magnetic correlations which is an evidence of frustration. The magnetic behavior similar to that observed in frustrated spin-glass system can be induced by such a frustration. Due to two kinds of magnetic interactions of about same order, a partial magnetic disorder can be also considered. In such a case, this magnetic phase seems to coexist with the antiferromagnetic nm sublattice, in a similar way to the coexistence with the superconducting behavior observed in Fe-doped $\text{YBa}_2\text{Cu}_3\text{O}_7$ and with the antiferromagnetic one in Fe-doped $\text{Bi}_4\text{Sr}_8\text{Cu}_5\text{O}_{19.8}$.^{21,22}

In conclusion, the magnetic irreversibility of $\text{Ca}_2\text{FeSbO}_6$ and $\text{Sr}_2\text{FeSbO}_6$ would be associated with a competition of antiferromagnetic and ferromagnetic interactions between two Fe(III) ions a distance $\sqrt{2}a_p$ apart which may introduce a spin frustration. $\text{Sr}_2\text{FeBiO}_6$ shows a spin-glass like behavior in the absence of chemical disorder which is indeed unusual. Although it is generally believed that, in order to observe spin-glass behavior, there must be some sort of disorder in the compound, this does not seem to be the case in ordered perovskite. Such a difference can be tentatively understood in terms of the partial cancellation of antiferromagnetic and ferromagnetic interactions which gives a frustration in magnetic sublattice. Until a definitive neutron diffraction and ac-susceptibility data are obtained, however, the question of the existence of real spin-glass phase in $\text{Sr}_2\text{FeBiO}_6$ must remain open. Further investigation of ord-

ered perovskite systems with d^{10} non-magnetic intermediary such as Sb^{5+} and Bi^{5+} may give some insight into the role that a competition between the nn and the nnn interaction in ordered cubic perovskite lattice plays in the spin-glass problem.

Acknowledgment. This paper was supported by NON DIRECTED RESEARCH FUND, Korea Research Foundation and Kyung Hee University.

References

1. Blasse, G. *J. Inorg. Nucl. Chem.* **1965**, 27, 993.
2. Goodenough, J. B.; Longo, J. M. *Landolt-Borenstein New Series, Vol. 4, Part a*; Springer-Verlag: Berlin, 1970.
3. Byeon, S. H.; Demazeau, G.; Choy, J. H.; Fournes, L. *Mater. Lett.* **1991**, 12, 163.
4. Byeon, S. H.; Nakamura, T.; Itoh, M.; Matsuo, M. *Mater. Res. Bull.* **1992**, 27, 1065.
5. Blasse, G. *J. Inorg. Nucl. Chem.* **1965**, 27, 993.
6. Izumi, F.; Murata, H.; Watanabe, N. *J. Appl. Cryst.* **1987**, 20, 411.
7. The crystallographic data can be ordered from corresponding author.
8. Cyrot, M. *Solid State Commun.* **1981**, 39, 1009.
9. Toulouse, G. *Comm. Phys.* **1977**, 2, 115.
10. Westerhold, K.; Bach, H. *J. Magn. Magn. Mater.* **1981**, 24, 191.
11. Binder, K.; Young, A. P. *Rev. Mod. Phys.* **1986**, 58, 801.
12. Rodriguez, R.; Fernandez, A.; Isalgue, A.; Rodriguez, J.; Labarta, A.; Tejada, J.; Obradors, X. *J. Phys. C* **1985**, 18, L401.
13. Westerhold, K.; Bach, H. *Phys. Rev. Lett.* **1981**, 47, 1925.
14. Westerhold, K.; Eiling, A.; Bach, H. *J. Magn. Magn. Mater.* **1982**, 28, 214.
15. Greedan, J. E.; Sato, M.; Yan, Xu; Razavi, F. S. *Solid State Comm.* **1986**, 59, 895.
16. Greedan, J. E.; Reimers, J. N.; Stager, C. V.; Penny, S. L. *Phys. Rev. B* **1991**, 43, 5682.
17. De Jongh, L. J.; Block, R. *Physica B* **1975**, 79, 568.
18. Blass, G. *Philips Res. Rept.* **1965**, 20, 327.
19. Mattheiss, L. F.; Hamann, D. R. *Phys. Rev. B* **1982**, 26, 2686.
20. Battle, P. D.; Goodenough, J. B.; Price, R. *J. Solid State Chem.* **1983**, 46, 234.
21. Diu, Z. Q.; Du, Y. W.; Tang, H.; Walker, J. C.; Bryder, W.; MorJani, K. *J. Magn. Magn. Mat.* **1987**, 69, 221.
22. Caldes, M. T.; Fuertes, A.; Bruna, Li.; Obradors, X.; Martnez, B.; Perez, F. *J. Appl. Phys.* **1991**, 70, 6184.